Journal of Neuroimmunology 276 (2014) 119–125

Contents lists available at ScienceDirect

Journal of Neuroimmunology

journal homepage: www.elsevier.com/locate/jneuroim

Origins of the sympathetic innervation to the nasal-associated lymphoid tissue (NALT): An anatomical substrate for a neuroimmune connection

Lucas E. Marafetti, Horacio E. Romeo *

Facultad de Ciencias Médicas, Pontificia Universidad Católica Argentina, Ciudad Autónoma de Buenos Aires C1107ADF, Argentina

ARTICLE INFO

Article history:
Received 11 May 2014
Received in revised form 2 September 2014
Accepted 4 September 2014

Keywords:
Nasal-associated lymphoid tissue
Superior cervical ganglia
Vesicular monamine transporter 2
Neuroimmune connection
Immunocytochemistry
Hamster

ABSTRACT

The participation of sympathetic nerve fibers in the innervation of the nasal-associated lymphoid tissues (NALT) was investigated in hamsters. Vesicular monoamine transporter 2 (VMAT2), an established sympathetic marker, is expressed in all neurons of superior cervical ganglia (SCG). In addition, VMAT2 -immunoreactive nerve fibers were localized in the NALT as well as in adjacent anatomical structures of the upper respiratory tract. Unilateral surgical ablation of the SCG abolished VMAT2 innervation patterns ipsilaterally while the contra lateral side is unaffected. These results provide the anatomical substrate for a neuroimmune connection in the NALT.

1. Introduction

The nasal mucosa is in the front line of defense against potential infections and the immune surveillance is brought by immune cell populations that transit to and from lymphoid tissues. In rodents, the mucosal immune defense of the nasal cavity consisted of a paired accretion of various lymphoid cells which are situated at the entrance of the nasal duct just dorsally to the soft palate (Spit et al., 1989; Kuper et al., 1990; Koornstra et al., 1991). This organized lymphoid tissue, connected with the respiratory epithelium, is denominated nasal-associated lymphoid tissue (NALT) and is the anatomical equivalent to the adenoid tonsil in humans (Koornstra et al., 1993). Both, the morphological structure as well as the immunological mechanisms of reaction, have been described and well characterized for a while in rodents (Hameleers et al., 1989; Giannasca et al., 1997; Hiroi et al., 1998; Zuercher and Cebra, 2002; Kiyono and Fukuyama, 2004). Due to their privileged anatomical placement, the NALT is constantly exposed to airborne antigenic substances and has been employed as an experimental model to scrutinize the infectivity of diverse pathogens. To investigate the local immune responses, the spread of infections or the histopathological changes in the NALT (Kuper, 2006), different species of rodents were experimentally challenged through the nasal conduit with diverse substances. Following several experimental protocols, strains of bacteria (Costalonga et al., 2009; Fernandez et al., 2011; Kim et al., 2011), virus (Wiley et al., 2005; Rudraraju et al., 2011) prions (Kincaid and Bartz, 2007; Kincaid et al., 2012), keyhole limpet hemocyanin (Hameleers et al., 1991), or nasal toxicants (Kuper et al., 2003) were nasally administrated and NALT responses were evaluated. Interestingly, the nasal route has been proposed as a less invasive passageway for vaccine administration where the NALT might play a key role in antibody defenses (Brandtzaeg, 2011; Kim et al., 2011).

Although all paravertebral sympathetic ganglia along the sympathetic chain are essentially similar, the anatomical location of the superior cervical ganglia (SCG) assigns them a peculiar degree of physiological relevance. The SCG are the uppermost ganglia of the paravertebral sympathetic chain and provide noradrenergic innervations to the skull, neck and facial structures (Cardinali and Romeo, 1991; Romeo et al., 2013). Several important structures are under SCG innervation territory including lymphoid tissues (Romeo et al., 1991, 1994; Esquifino and Cardinali, 1994). Despite that human existing data is restricted to palatine tonsils (Ueyama et al., 1990; Weihe and Krekel, 1991), the presence and origins of nerve fibers in the rodent NALT are still unseen. Therefore, the confirmation for the conceivable sympathetic innervation to the NALT arising from the SCG should be addressed.

Previous studies have revealed that cervical sympathetic fibers are capable of modulating the local immune response (Alito et al., 1987; Romeo et al., 1991) and, therefore, could be involved in NALT immune performances. In addition, the presence and distribution of sympathetic nerve fibers gain importance due to the fact that prions infecting the

* Corresponding author at: Facultad de Ciencias Médicas, Pontificia Universidad Católica Argentina, Alicia Moreau de Justo 1500, 4to piso, C1107ADF CABA, Argentina. Tel./fax: +54 11 4349 0200.
E-mail address: horacio_romeo@uca.edu.ar (H.E. Romeo).

http://dx.doi.org/10.1016/j.jneuroim.2014.09.003
0165-5728/

nasal cavity of the hamster (Kincaid and Bartz, 2007; Kincaid et al., 2012) might use this neural route to invade the central nervous system.

Vesicular monoamine amine transporters (VMAT) are key transport membrane proteins that allocate the passage of catecholamines and serotonin inside the synaptic vesicles of monoaminergic neurons (Erickson et al., 1996). In particular, the existence of the isoform VMAT2 has been recognized in almost all aminergic neurons (Erickson et al., 1992; Liu et al., 1992). Indeed, antibodies against VMAT2 are reliable immunocytochemical markers to specify and visualize sympathetic nerve fibers and neurons (Weihe et al., 1994; Peter et al., 1995; Hou and Dahlström, 1996; Weihe and Eiden, 2000). Besides for mice and rats, VMAT2 immunocytochemistry has not been utilized to reveal detailed innervation patterns in other rodent species.

Given that the sympathetic innervation plays a crucial role in modulating and regulating immune responses (Nance and Sanders, 2007), we aimed to indentify the origins of the sympathetic fibers that innervate the NALT and surrounding tissues of the upper respiratory tract. In the present study, we employed the hamster as an experimental model to explore for the first time the origins and distribution of the sympathetic innervation to the NALT in a rodent species.

The hypothesis to be attested is that postganglionic nerve fibers arising from the SCG penetrate the NALT and also innervate other anatomical structures of the upper respiratory tract. Moreover, each SCG will be confined to a restricted ipsilateral innervation territory. A plausible connection between nerve fibers and immune cells inside the NALT is also envisaged.

In order to address the origin of the sympathetic innervation to the NALT as well as the distribution of sympathetic fibers on adjacent anatomical structures of the upper respiratory tract, we employed highly sensitive immunocytochemical techniques using VMAT2 antibodies followed by quantitative analysis and straightforward microsurgical procedures.

2. Materials and methods

2.1. Subjects

Male Syrian hamsters (*Mesocricetus auratus*) weighing an average of 90 g were employed in the present study. The animals (n = 12) were kept under constant light conditions in a 12:12 light:dark cycle and were given access to food and water ad libitum at UCA animal facilities. The use of animals was in accordance with the National Institutes of Health Guidelines for the Care and Use of Laboratory Animals and approved by the Animal Research Committee at UCA.

2.2. Superior cervical ganglionectomy (SCGx)

Groups of hamsters were randomly assigned to surgical removal of the superior cervical ganglia (SCGx). Surgeries were performed, bilaterally (SCGx bil, n = 2), unilaterally (SCGx unil, n = 6) or sham operation (n = 4) following a similar procedure standardized in rats (Savastano et al., 2010; Romeo et al., 2013). Briefly, animals were anesthetized with Equithesin (4.6% choral hydrate, 0.97% pentobarbitone, 2.1% magnesium sulfate and 9% ethanol in aqueous solution) and were placed supine on a heating pad. The level of responsiveness to the anesthesia was monitored by toe pinching. While the animal was completely sedated, the ventral surface of the neck was shaved with clippers and rinsed preoperatively with Povidona iodide. Through a 1.5 cm vertical incision on the skin, the salivary glands were exposed and then retracted to gain access to sternohyoid and omohyoid muscles. By using microdissecting scissors the omohyoid muscle was carefully dissected and the superior cervical ganglion (SCG) was visualized at the bifurcation of the common carotid artery. The ganglia were carefully ablated unilaterally or bilaterally by employing microsurgical forceps. This dissection procedure was done cautiously in order to maintain the anatomical integrity of the SCG for immunocytochemical assessment. For sham operations the same surgical approach was employed except for when the SCG was removed. The surgical procedure was completed when the wound was cleansed and then closed with 4–0 monofilament Nylon sutures. After recovering from anesthesia animals were placed individually in cages. The criterion employed to validate the effectiveness of the surgical procedures is the irreversible ptosis, bilateral or unilateral depending upon the experimental group, commencing to manifest from 30 hs after surgery (Savastano et al., 2010; Romeo et al., 2013).

2.3. Tissue preparation

SCG obtained from SCGx were immersed in Bouin's solution for 24 h. Additionally, four animals with bilateral sham operations were decapitated under Equithesin anesthesia and the SCG were rapidly removed and fixed in the same solution.

Ten days after cervical surgeries, the animals were deeply anesthetized and decapitated. After removal of the lower jaw, the nose was cut lengthwise into equal halves. Lymphoid structures and surrounding tissues of the upper respiratory tract were carefully dissected under a stereoscopic microscope (Zeiss Optiflex) using microsurgical forceps and scissor. The nasal-associated lymphoid tissues (NALT) are located at the entrance of the nasopharyngeal duct. After dissection, tissues were immediately immersed in Bouin's solution fixative for 24 h. Following fixation, all the specimens (SCG and lymphoid structures) were washed for several days in ethanol 70% until picric acid was removed, dehydrated and embedded in paraffin. Sections were cut at 7–10 μm with a sliding microtome and placed on gelatinized glass slides.

2.4. Immunocytochemical procedures

Deparaffinized sections were rehydrated and, in order to quench endogenous peroxide activity, were treated with 3% H_2O_2 in methanol for 30 min. To improve the immunocytochemical detection, sections were washed in distilled water and then heated at 94–95 °C in 0.01 M citrate buffer (pH 6) for 10 min. The nonspecific antibody binding was blocked by incubation in 5% horse serum in phosphate-buffered saline (PBS) (10 mM, 7.4 pH) for 30 min and then washed with PBS for 10 min. Sections were incubated in a 1:1500 working dilution with rabbit anti-VMAT2 primary antibody directed to C-termini (Chemicon, # AB1767, lot: LV1359414, Temecula, California) overnight at 15 °C followed by 2 h at 37 °C. After several washes in PBS sections were incubated with a biotinylated secondary antibody (Vectastain ABC Kit SK- 6200, Vector Laboratories, Burlingame, California) for 45 min at 37 °C followed by 2 washes in PBS and then incubated in avidin–biotin–peroxidase complex (Vectastain ABC Kit, SK-6200, Vector Laboratories) for 1 h at 37 °C. Finally, after several washes with PBS, immunoreactions were visualized by an enzymatic reaction with diaminobenzidine (DAB) as chromogen and nickel sulfate enhance (Vector DAB substrate kit, SK-4100, Vector Laboratories) in PBS containing 0.003% H_2O_2, resulting in an insoluble black precipitate product. In specificity controls for the immunoreactions the primary antibody, the secondary antibody or the ABC complex were omitted. There was no evidence for nonspecific immunoreactions. Sections were washed, dehydrated in graded ethanol-xylene, and mounted with Depex under glass coverslips.

2.5. Documentation and analysis

Photodocumentation was performed using a Nikon Eclipse 50i light microscope with an attached digital camera Nikon DS-Ri1 (Nikon Instruments Inc.).

In order to evaluate the density of VMAT2 immunoreactive (VMAT2-ir) nerve fibers on the NALT and adjacent tissues of the upper respiratory tract, the images were digitalizing and assessed by densitometry using the Image J 1.4 software (NIH, USA) on a personal computer. In randomly sampled sections of SCGx and sham animals,

the areas of defined anatomical structures were measured. Inside each delimited area, the nerve fiber corresponding area was also calculated and measured. The nerve fibers density was expressed as a relation between the total area of each particular structure and the total area occupied by the nerve fibers. Intergroup differences in innervation density between SCGx and Sham were evaluated using the independent sample Student t test. A *P* value of less than 0.05 was considered statistically significant.

3. Results

Clusters of strongly positive and less positive sympathetic neurons for VMAT2 were found throughout the entire SCG and were randomly distributed between the rostral and caudal poles of the ganglion (Fig. 1A). VMAT2 immunostaining was scattered in the cytoplasm of perikarya as well as in cell processes (Fig. 2B). Similar findings but, constrained to rats, were previously reported (Weihe et al., 1994; Peter et al., 1995; Hou and Dahlström, 1996; Headley et al., 2007). The omission of VMAT2 primary and/or secondary antibodies during the incubation protocol resulted in the lack of immunoreactivity (data not shown).

After predicting a sympathetic origin, we investigated the presence and distribution of VMAT2-immunoreactive (VMAT2-ir) nerve fibers at microanatomical locations of upper respiratory tract related to the NALT (Fig. 2A). VMAT2-ir nerve fibers formed dense bundles of varicosities that were distributed among the blood vessels. Less frequent nerve fibers were found in the subepithelial layer and fibers were completely absent in the respiratory epithelia (Fig. 2B). The VMAT2 innervation patterns identified are consistent with patterns of a sympathetic phenotype. Compared with other adjacent tissues of the upper respiratory tract, VMAT2-ir nerve fibers were scarce in the NALT (Fig. 3B and C). Nerve fibers were found surrounding the small intra-NALT blood vessels (Fig. 3B), as well as branched off among lymphoid cells (Fig. 3D). The light microscopy technique employed here is not sensitive enough to determine whether nerve fibers make synaptic contact with cells of the NALT (Fig. 3D).

Microsurgical ablations of the SCG provided the confirmation on the origins of VMAT2-ir fibers that innervates the NALT and adjacent tissues of the upper respiratory tract. Unilateral SCGx abolished VMAT2 innervation patterns when compared to the contra lateral side that includes the unhurt SCG (Fig. 4). No VMAT2-ir nerve fibers were visualized after bilateral SCGx (data not shown). The restricted ipsilateral innervation pathways of the sympathetic projections were evaluated by densitometry on the different microanatomical structures and corroborated the disappearance of VMAT2-ir nerve fibers after the surgery (Table 1).

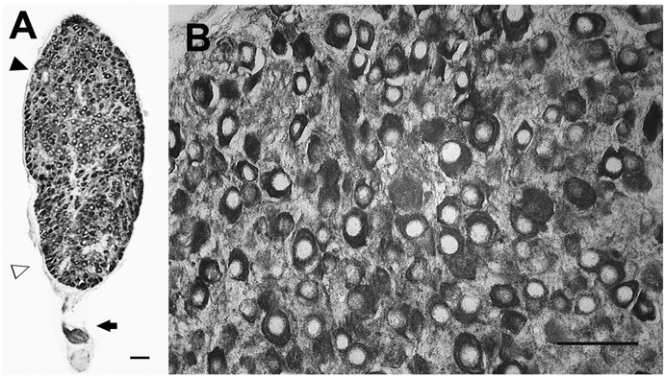

Fig. 1. Expression of VMAT2 immunoreactivity in SCG. Low-power light micrograph demonstrating the presence of VMAT2-ir neurons contained along the entire structure of the SCG (A). The cervical sympathetic trunk (CST, complete arrow), rostral portion (black arrow head) and caudal portion (white arrow head) of the SCG are designated. High-power light micrograph of SCG perikarya exhibiting variable intensities of immunostaining for VMAT2 (B). Scale bars represent 100 μm in A and 50 μm in B.

4. Discussion

In the present study, our hypothesis that postganglionic nerve fibers arising from the SCG penetrate the NALT and also innervate other anatomical structures of the upper respiratory tract is sustained by the experimental evidence shown. The SCGx completely obliterated the detection of VMAT2-ir in the NALT as well as in the adjacent tissues. Moreover, as the unilateral microsurgical ablation of the SCGx has confirmed, the innervation territory for each SCG is strictly ipsilateral. Additionally, it is worth noting that this study represents the first reported demonstration about the occurrence of nerve fibers in the NALT.

Two isoforms of the vesicular monoamine transporter (VMAT) were isolated with molecular cloning techniques from different tissues or cell lines (Erickson et al., 1992; Liu et al., 1992). Both transporters although related, are functionally different (Peter et al., 1994). VMAT1 is expressed solely in endocrine cells of the intestine, stomach, adrenal medulla and small intensely fluorescent cells in sympathetic ganglia (Weihe et al., 1994). Contrastingly VMAT2 that is expressed in monoaminergic neurons, has been widely employed as a reliable immunocytochemical marker for sympathetic neurons and nerve fibers (Weihe et al., 1994; Peter et al., 1995; Erickson et al., 1996; Hou and Dahlström, 1996; Weihe and Eiden, 2000; Headley et al., 2007). Indeed, the coexistence of VMAT2 and tyrosine hydroxylase (TH) immunoreactivities was confirmed in neurons of both paravertebral and prevertebral sympathetic chains of rats (Weihe and Eiden, 2000). The present study demonstrated that the vast majority of neurons in the SCG of the hamster are positive for VMAT2 whereas the immunostaining is distributed mainly in the cytoplasm of perikarya and in cell processes. There was no difference between the rostral and caudal poles of the SCG regarding neuron's staining intensity. Few VMAT2-ir nerve fibers and varicosities were seen however, many were certainly masked by the intense immunostaining of neurons. Similar results, but restricted to rats, were previously reported (Weihe et al., 1994; Peter et al., 1995; Hou and Dahlström, 1996; Headley et al., 2007). Although in hamsters SCG neurons exhibiting a robust immunostaining for VMAT2 are preponderant, few of them displayed variable intensities. The basis for the differential intensity of VMAT2 immunostaining of neurons can only be speculated. It has been proposed that the expression of VMAT2 and the ensuing intensity of the immunostaining depend upon different functional subclasses of neurons reflecting diverse physiological states in the subcellular processing of the vesicular transporter (Headley et al., 2007). While out of the scope of our study, whether the variability in VMAT2 immunostaining reveals any physiological condition or are due to detection threshold of the immunochemical technique awaits further investigation.

VMAT2-ir nerve fibers and varicosities were found predominately surrounding the different types of blood vessels in the microanatomical structures of the upper respiratory tract adjacent to the NALT. We did not discriminate among the small arteries, arterioles, small veins or venules considered all together as the blood vessels. In fact, VMAT2-ir nerve fibers that supply innervation to the vasculature were previously located in the intestine (Weihe et al., 1994; Peter et al., 1995), the urinary bladder (Weihe and Eiden, 2000) and the submandibular salivary gland (Peter et al., 1995; Headley et al., 2007) of rats. Co-localization immunocytochemical studies performed on the blood vessels employing antibodies against VMAT2, TH and neuropeptide Y (NPY) clearly suggested the phenotype of those nerve fibers as sympathetic (Weihe and Eiden, 2000; Headley et al., 2007). While sparse, VMAT2-ir nerve fibers are scattered in the subepithelial layer but are completely absent in the epithelia of the upper respiratory tract adjacent to the NALT. A similar pattern involving rare fibers in the mucosa and non in the epithelia is present in the intestines of rats (Weihe et al., 1994).

Early immune studies before the introduction of VMAT2 immunocytochemistry have examine innervation patterns in the nasal mucosa. Assisted by the available antibodies, sympathetic, parasympathetic and sensory nerve fibers arising from different sources were detected

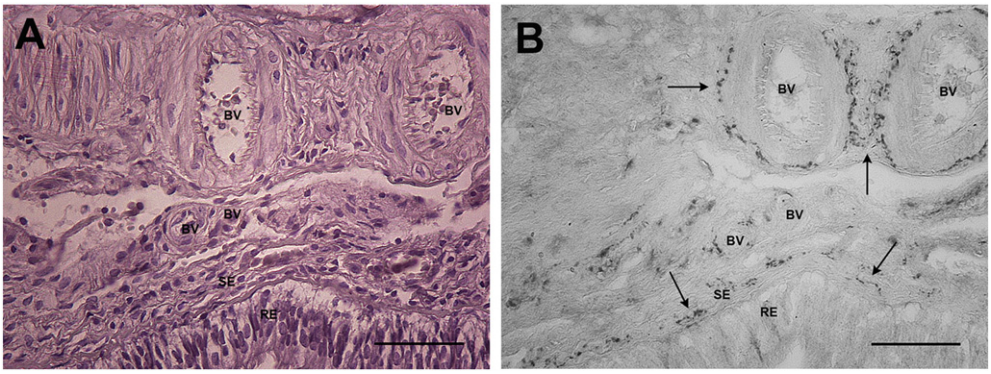

Fig. 2. Expression and distribution of VMAT2-ir nerve fibers in some microanatomical structures of the upper respiratory tract. High-power light micrographs of consecutive sections, stained with hematoxylin and eosin (A) and immunocytochemistry for VMAT2 (B) pointing positive nerve fibers (arrows). Besides on the RE (respiratory epithelium), VMAT2-immunoreactive nerve fibers are widespread over the different structures. BV = blood vessels, SE = subepithelial layer. Scale bars represent 50 μm.

in the turbinate mucosa and the septum (Uddman et al., 1983; Lacroix et al., 1990; Amores et al., 1991), Nevertheless and probably due to it peculiar anatomical location, the upper respiratory tract with the accompanying NALT has been overlooked. Chemical noradrenergic denervation with 6-hidroxydopamine (6-OHDA) completely eradicates the sympathetic innervation in the nasal mucosa after the neurotoxin was administered intranasally (Amores et al., 1991). Interestingly, unilateral SCG only abolish sympathetic innervation in the ipsilateral side of the nasal mucosa (Lacroix et al., 1990; Amores et al., 1991). Taking into account anatomical features, a similar consideration was anticipated to VMAT2-ir nerve fibers in the upper respiratory tract of hamsters. Conclusively, the densitometry analysis further demonstrated an absolute obliteration of VMAT2 immunoreactivity on the different scrutinized areas after unilateral or bilateral SCGx.

Another approach to elucidate the anatomical origin of a given innervation path is the employment of neuronal tracing. Experiments injecting a retrograde tracer into the anterior-lateral part of the nasal mucosa were carried out to identify the anatomical settlement of the projecting neuronal bodies (Grunditz et al., 1994). Labeled neurons came upon in the SCG, the sphenopalatine ganglia and the trigeminal ganglia of the ipsilateral side of the tracing injection. However, a few neurons were also labeled in the contralateral ganglia. In the same paper, unilateral SCGx emerged to sustain tracing data (Grunditz et al., 1994). It is worth to note that conclusions of neuronal tracing experiments must be interpreted with caution. For instance, tracing substances may leak outside the injection place especially in mucosal tissues; therefore neurons belonging to another innervation territory could be labeled. On the other hand, if the tracer did not completely penetrate the target tissue the number of projecting neurons might be unrepresented (Hunter and Dey, 1998).

The anatomical location of the NALT, turn out to be a technically challenging place for a direct injection of retrograde tracer. However

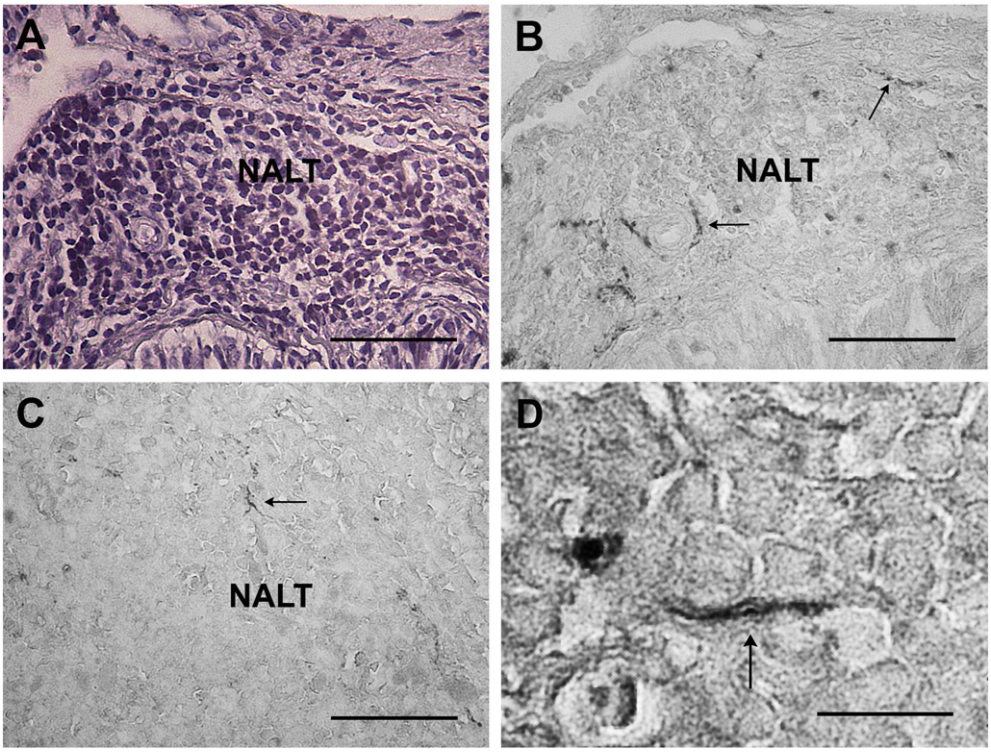

Fig. 3. Presence and distribution of VMAT2-ir nerve fibers in the nasal-associated lymphoid tissue. High-power photomicrographs of NALT in consecutive sections stained with hematoxylin and eosin (A) and immunocytochemistry for VMAT2 (B). Arrows indicate the existence of VMAT2-ir nerve fibers in different sections of NALT (A, C). High-power light micrograph pointing VMAT2-ir nerve fibers (arrow) that passes through cells inside the NALT (D). Scale bar represents 50 μm.

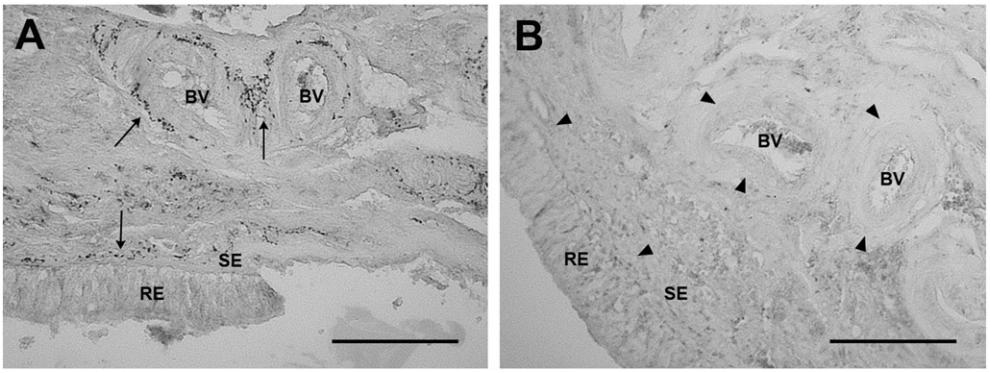

Fig. 4. Effect of unilateral SCGx on different microanatomical structures of the upper respiratory tract associated to NALT. High-power light micrographs of normal innervated (A), and denervated by unilateral SCGx (B) obtained from the same animal. Note the presence and distribution of VMAT2-ir nerve fibers (A), and the roughly entire disappearance of nerve fibers after the surgery (B). Arrows (VMAT2-ir nerve fibers) and arrowheads (lack of nerve fibers) point to similar microanatomical structures (A, B). BV = blood vessels, SE = subepithelial layer, RE = respiratory epithelium. Scale bar represents 100 μm.

and more critical, it is quite impossible to avoid any leak of the tracer from the mucosal associated-lymphoid tissue to surrounding structures. Few authors have performed retrograde tracing on different lymphoid tissues such thymus (Nance et al., 1987; Trotter et al., 2007), spleen (Nance and Burns, 1989; Cano et al., 2001) and lymph nodes (Kurkowski et al., 1990; Romeo et al., 1994). Moreover, due to the fact that those lymphoid tissues are encapsulated and cautious injection procedures, the tracer did not escape outside the desire structure and allowed reliable retrograde tracing results. In contrast, since the close contact between mineralized bone and the bone marrow, the origin of the innervation of bone marrow revealed by retrograde tracer is still controversial (Denes et al., 2005).

Considering our neuroanatomical experience upon lymphoid organs (Romeo et al., 1994) that support the complicatedness and limitations of retrograde tracing on mucosal associated tissues, we attempted neuronal tracing employing the recognized retrograde and anterograde tracer Fluoro Ruby (FR). By exploiting its anterograde capability, FR was carefully injected in the SCG. Days after the injection very few FR-containing nerve fibers and restricted to the ipsilateral upper respiratory tract were detected (unpublished results). Unfortunately and due to background setbacks, we were unable to identify the microanatomical structures where those FR-containing nerve fibers might be distributed. Following these discouraging results, we decided to continue with the available immunocytochemical and microsurgical approaches.

The crucial finding in our report is the occurrence of sympathetic nerve fibers recognized by it VMAT2 phenotype in the NALT of hamsters. The sympathetic innervation has been documented in diverse mucosal-associated lymphoid tissues (MALT), such as bronchus-associated lymphoid tissue (BALT) (Nohr and Weihe, 1991) or Gut-associated lymphoid tissue (GALT) where nerve fibers may play a role during intestinal inflammation (Straub et al., 2006). Sympathetic nerve fibers participate in the modulation of the local immune response acting at two different levels concurrently. Directly, by neurotransmitters interacting on their respective receptors present in immune competent cells (Kin and Sanders, 2006; Sanders, 2012) or indirectly, by regulating the blood flow in lymphoid compartments (Rogausch et al., 2004). Indeed, we found that VMAT2-ir nerve fibers run through NALT lymphoid cells but also innervates the intra-NALT blood vessels. A direct experimental proof upon a plausible modulatory role of the sympathetic innervation on NALT is lacking. Moreover, although VMAT2 nerve fibers run through and/or make contact with lymphocytes the immune phenotype of those NALT cells remain to be revealed. The anatomical relation between nerve fibers and characterized populations of immune cells by combined dual labeling immunocytochemical techniques is currently under investigation in our laboratory. Nevertheless, over the past two decades the accumulated evidence supports an inhibitory action of the sympathetic innervation on both innate and adaptive immunities (Nance and Sanders, 2007). Paired NALT would be a useful experimental model to investigate induced immune responses using the same animal as the proper control. For instance, when paired lymphoid organs such lymph nodes are involved, local immune responses can be unilaterally manipulated (Alito et al., 1987; Romeo et al., 1991). Whether functional changes in the sympathetic activity such as an increase or decrease in the release of neurotransmitters would affect the immune responses in the NALT deserves further investigation. We are well aware that the present study is constrained to the sympathetic pathway to the NALT. Other conceivable sources of nerve fibers such as parasympathetic and/or sensory are not ruled out, and are currently under investigation in our laboratory.

The nasal cavity in hamsters is one route for the entrance of prions and the initial accumulation site of the infection is precisely located in NALT (Kincaid and Bartz, 2007; Sbriccoli et al., 2009; Kincaid et al., 2012). Nonetheless, most studies connecting prions infection and nerve carrying on of the disease comprehended the enteric nervous system (Chiocchetti et al., 2008). Following oral administration of prions, pathological deposition of proteins related to prions was detected in the sympathetic coeliac mesenteric ganglion complex as well as in other neural structures (Mc Bride and Beekes, 1999). Moreover, the participation of sympathetic neural pathways in the spread of the infection was suggested by experiments with 6-OHDA. Chemical sympathectomy considerably delayed the onset of the disease in animals challenged with prions (Glatzel et al., 2001). Whether the VMAT2 sympathetic nerve fibers of the NALT are conceivable but presently an unknown route for prions infection, and whether the SCG could operate as a relay station from where prions would propagate to the central nervous

Table 1
Densitometry analysis of VMAT2-ir nerve fibers in SCGx or Sham operated animals performed on different microanatomical structures of the upper respiratory tract and the NALT.

	SCGx	Sham	T	*P* value
Subepithelial layer	0.0014 ± 0.0001 (n = 6)	0.0063 ± 0.0004 (n = 11)	10.28	0.0001
Blood vessels	0.0001 ± 0.0000 (n = 6)	0.0190 ± 0.0013 (n = 6)	13.68	0.0001
NALT	0.0002 ± 0.0000 (n = 6)	0.0011 ± 0.0001 (n = 6)	5.39	0.003

Data are expressed as mean ± SE of the relation between the area containing the nerve fibers/the total area corresponding to each microanatomical structure. *P* values are statistically very significant.

system are still motivating open questions to be undertaken in future investigations.

5. Conclusions

Taken together, the current data provides the anatomical substrate for a neuroimmune connection in the NALT of hamsters. The bi-directional connection would transmit information from the central nervous system to the peripheral NALT and vice versa using sympathetic channels. By an anterograde trend sympathetic nerve fiber might influence the local immune responses in the NALT while retrogradely, would served as the route to convey information of local immune challenges to the central nervous system. We also speculate on the potential participation of cervical sympathetic fibers in the dissemination of prions disease to central nervous structures. The existence of the sympathetic route does not invalidate the participation of non-sympathetic nerve fibers projecting to the NALT. Further characterizations of the neuroimmune connections in the NALT should provide insight in the pathophysiology of the nasal cavity.

Acknowledgments

This study contains parts of the thesis of L. E. Marafetti. We express our acknowledgment to Dr. Pablo Scacchi-Bernasconi, Dr. Daniel Navacchia and Mrs. Silvia Scordomaglia for their skillful technical assistance. Research was supported by a grant from CONICET to H.E. Romeo (PIP-CONICET 114-20080100100).

References

Alito, A.E., Romeo, H.E., Baler, R., Chuluyan, H.E., Braun, M., Cardinali, D.P., 1987. Autonomic nervous system regulation of murine immune responses as assessed by local surgical sympathetic and parasympathetic denervation. Acta Physiol. Pharmacol. Latinoam. 37, 305–319.

Amores, A.E., Sprekelsen, C., Bernal-Sprekelsen, M., 1991. Immunoreactive nerve fibers in the nasal mucosa. An experimental study on neuropeptides Y, calcitonin gene-related peptide and galanin. Eur. Arch. Otorhinolaryngol. 248, 487–491.

Brandtzaeg, P., 2011. Potential of nasopharynx-associated lymphoid tissue for vaccine responses in the airways. Am. J. Respir. Crit. Care Med. 183, 1595–1604.

Cano, G., Sved, A.F., Rinaman, L., Rabin, B.S., Card, J.P., 2001. Characterization of the central nervous system innervation of the rat spleen using viral transneuronal tracing. J. Comp. Neurol. 439, 1–18.

Cardinali, D.P., Romeo, H.E., 1991. The autonomic nervous system of the cervical region as a channel of neuroendocrine communication. Front. Neuroendocrinol. 12, 278–297.

Chiocchetti, R., Mazzuoli, G., Albanese, V., Mazzoni, M., Clavenzani, P., Lalatta-Costerbosa, G., Lucchi, M.L., Di Guardo, G., Marruchella, G., Furness, J.B., 2008. Anatomical evidence for ileal Peyer's patches innervation by enteric nervous system: a potential route for prion neuroinvasion? Cell Tissue Res. 332, 185–194.

Costalonga, M., Cleary, P.P., Fischer, L.A., Zhao, Z., 2009. Intranasal bacteria induce Th1 but not Treg or Th2. Mucosal Immunol. 2, 85–95.

Denes, A., Boldogkoi, Z., Uhereczky, G., Hornyak, A., Rusvai, M., Palkovits, M., Kovacs, K.J., 2005. Central autonomic control of the bone marrow: multisynaptic tract tracing by recombinant pseudorabies virus. Neuroscience 134, 947–963.

Erickson, J.D., Eiden, L.E., Hoffman, B.J., 1992. Expression cloning of a reserpine-sensitive vesicular monoamine transporter. Proc. Natl. Acad. Sci. U. S. A. 89, 10993–10997.

Erickson, J.D., Schafer, M.K., Bonner, T.I., Eiden, L.E., Weihe, E., 1996. Distinct pharmacological properties and distribution in neurons and endocrine cells of two isoforms of the human vesicular monoamine transporter. Proc. Natl. Acad. Sci. U. S. A. 93, 5166–5171.

Esquifino, A.I., Cardinali, D.P., 1994. Local regulation of the immune response by the autonomic nervous system. Neuroimmunomodulation 1, 265–273.

Fernandez, S., Cisney, E.D., Hall, S.I., Ulrich, R.G., 2011. Nasal immunity to staphylococcal toxic shock is controlled by the nasopharynx-associated lymphoid tissue. Clin. Vaccine Immunol. 18, 667–675.

Giannasca, P.J., Boden, J.A., Monath, T.P., 1997. Targeted delivery of antigen to hamster nasal lymphoid tissue with M-cell-directed lectins. Infect. Immun. 65, 4288–4298.

Glatzel, M., Heppner, F.L., Albers, K.M., Aguzzi, A., 2001. Sympathetic innervation of lymphoreticular organs is rate limiting for prion neuroinvasion. Neuron 31, 25–34.

Grunditz, T., Uddman, R., Sundler, F., 1994. Origin and peptide content of nerve fibers in the nasal mucosa of rats. Anat. Embryol. 189, 327–337.

Hameleers, D.M., van der Ende, M., Biewenga, J., Sminia, T., 1989. An immunohistochemical study on the postnatal development of rat nasal-associated lymphoid tissue (NALT). Cell Tissue Res. 256, 431–438.

Hameleers, D.M., van der Ven, I., Biewenga, J., Sminia, T., 1991. Mucosal and systemic antibody formation in the rat after intranasal administration of three different antigens. Immunol. Cell Biol. 69, 119–125.

Headley, D.B., Suhan, N.M., Horn, J.P., 2007. Different subcellular distributions of the vesicular monoamine transporter, VMAT2, in subclasses of sympathetic neurons. Brain Res. 1129, 156–160.

Hiroi, T., Iwatani, K., Iijima, H., Kodama, S., Yanagita, M., Kiyono, H., 1998. Nasal immune system: distinctive Th0 and Th1/Th2 type environments in murine nasal-associated lymphoid tissues and nasal passage, respectively. Eur. J. Immunol. 28, 3346–3353.

Hou, X.E., Dahlström, A., 1996. Synaptic vesicle proteins in cells of the sympathoadrenal lineage. J. Auton. Nerv. Syst. 61, 301–312.

Hunter, D.D., Dey, R.D., 1998. Identification and neuropeptide content of trigeminal neurons innervating the rat nasal epithelium. Neuroscience 83, 591–599.

Kim, D.Y., Sato, A., Fukuyama, S., Sagara, H., Nagatake, T., Kong, I.G., Goda, K., Nochi, T., Kunisawa, J., Sato, S., Yokota, Y., Lee, C.H., Kiyono, H., 2011. The airway antigen sampling system: respiratory M cells as an alternative gateway for inhaled antigens. J. Immunol. 186, 4253–4262.

Kin, N.W., Sanders, V.M., 2006. It takes nerve to tell T and B cells what to do. J. Leukoc. Biol. 79, 1093–1104.

Kincaid, A.E., Bartz, J.C., 2007. The nasal cavity is a route for prion infection in hamsters. J. Virol. 81, 4482–4491.

Kincaid, A.E., Hudson, K.F., Richey, M.W., Bartz, J.C., 2012. Rapid transepithelial transport of prions following inhalation. J. Virol. 86, 12731–12740.

Kiyono, H., Fukuyama, S., 2004. NALT- versus Peyer's-patch-mediated mucosal immunity. Nat. Rev. Immunol. 4, 699–710.

Koornstra, P.J., de Jong, F.I., Vlek, L.F., Marres, E.H., van Breda Vriesman, P.J., 1991. The Waldeyer ring equivalent in the rat. A model for analysis of oronasopharyngeal immune responses. Acta Otolaryngol. 111, 591–599.

Koornstra, P.J., Duijvestijn, A.M., Vlek, L.F., Marres, E.H., van Breda Vriesman, P.J., 1993. Immunohistochemistry of nasopharyngeal (Waldeyer's ring equivalent) lymphoid tissue in the rat. Acta Otolaryngol. 113, 660–667.

Kuper, C.F., 2006. Histopathology of mucosa-associated lymphoid tissue. Toxicol. Pathol. 34, 609–615.

Kuper, C.F., Hameleers, D.M., Bruijntjes, J.P., van der Ven, I., Biewenga, J., Sminia, T., 1990. Lymphoid and non-lymphoid cells in nasal-associated lymphoid tissue (NALT) in the rat. An immuno- and enzyme-histochemical study. Cell Tissue Res. 259, 371–377.

Kuper, C.F., Arts, J.H., Feron, V.J., 2003. Toxicity to nasal-associated lymphoid tissue. Toxicol. Lett. 140–141, 281–285.

Kurkowski, R., Kummer, W., Heym, C., 1990. Substance P-immunoreactive nerve fibers in tracheobronchial lymph nodes of the guinea pig: origin, ultrastructure and coexistence with other peptides. Peptides 11, 13–20.

Lacroix, J.S., Anggård, A., Hökfelt, T., O'Hare, M.M., Fahrenkrug, J., Lundberg, J.M., 1990. Neuropeptide Y: presence in sympathetic and parasympathetic innervation of the nasal mucosa. Cell Tissue Res. 259, 119–128.

Liu, Y., Peter, D., Roghani, A., Schuldiner, S., Privé, G.G., Eisenberg, D., Brecha, N., Edwards, R.H., 1992. A cDNA that suppresses MPP+ toxicity encodes a vesicular amine transporter. Cell 70, 539–551.

Mc Bride, P.A., Beekes, M., 1999. Pathological PrP is abundant in sympathetic and sensory ganglia of hamsters fed with scrapie. Neurosci. Lett. 265, 135–138.

Nance, D.M., Burns, J., 1989. Innervation of the spleen in the rat: evidence for absence of afferent innervation. Brain Behav. Immun. 3, 281–290.

Nance, D.M., Sanders, V.M., 2007. Autonomic innervation and regulation of the immune system (1987–2007). Brain Behav. Immun. 21, 736–745.

Nance, D.M., Hopkins, D.A., Bieger, D., 1987. Re-investigation of the innervation of the thymus gland in mice and rats. Brain Behav. Immun. 1, 134–147.

Nohr, D., Weihe, E., 1991. The neuroimmune link in the bronchus-associated lymphoid tissue (BALT) of cat and rat: peptides and neural markers. Brain Behav. Immun. 5, 84–101.

Peter, D., Jimenez, J., Liu, Y., Kim, J., Edwards, R.H., 1994. The chromaffin granule and synaptic vesicle amine transporters differ in substrate recognition and sensitivity to inhibitors. J. Biol. Chem. 269, 7231–7237.

Peter, D., Liu, Y., Sternini, C., de Giorgio, R., Brecha, N., Edwards, R.H., 1995. Differential expression of two vesicular monoamine transporters. J. Neurosci. 15, 6179–6188.

Rogausch, H., Böck, T., Voigt, K.H., Besedovsky, H., 2004. The sympathetic control of blood supply is different in the spleen and lymph nodes. Neuroimmunomodulation 11, 58–64.

Romeo, H.E., Colombo, L.L., Esquifino, A.I., Rosenstein, R.E., Chuluyan, H.E., Cardinali, D.P., 1991. Slower growth of tumours in sympathetically denervated murine skin. J. Auton. Nerv. Syst. 32, 159–164.

Romeo, H.E., Fink, T., Yanaihara, N., Weihe, E., 1994. Distribution and relative proportions of neuropeptide Y- and proenkephalin-containing noradrenergic neurones in rat superior cervical ganglion: separate projections to submaxillary lymph nodes. Peptides 15, 1479–1487.

Romeo, H.E., Savastano, L., Cardinali, D.P., 2013. Superior cervical ganglionectomy in rodents. In: Turgut, M. (Ed.), Step by Step Experimental Pinealectomy Techniques in Animals for Researchers. Nova Science Publishers Inc., New York, pp. 153–170.

Rudraraju, R., Surman, S., Jones, B., Sealy, R., Woodland, D.L., Hurwitz, J.L., 2011. Phenotypes and functions of persistent Sendai virus-induced antibody forming cells and CD8+ T cells in diffuse nasal-associated lymphoid tissue typify lymphocyte responses of the gut. Virology 410, 429–436.

Sanders, V.M., 2012. The beta2-adrenergic receptor on T and B lymphocytes: do we understand it yet? Brain Behav. Immun. 26, 195–200.

Savastano, L.E., Castro, A.E., Fitt, M.R., Rath, M.F., Romeo, H.E., Muñoz, E.M., 2010. A standardized surgical technique for rat superior cervical ganglionectomy. J. Neurosci. Methods 192, 22–33.

Sbriccoli, M., Cardone, F., Valanzano, A., Lu, M., Graziano, S., De Pascalis, A., Ingrosso, L., Zanusso, G., Monaco, S., Bentivoglio, M., Pocchiari, M., 2009. Neuroinvasion of the 263 K scrapie strain after intranasal administration occurs through olfactory-unrelated pathways. Acta Neuropathol. 117, 175–184.

Spit, B.J., Hendriksen, E.G., Bruijntjes, J.P., Kuper, C.F., 1989. Nasal lymphoid tissue in the rat. Cell Tissue Res. 255, 193–198.
Straub, R.H., Wiest, R., Strauch, U.G., Härle, P., Schölmerich, J., 2006. The role of the sympathetic nervous system in intestinal inflammation. Gut 55, 1640–1649.
Trotter, R.N., Stornetta, R.L., Guyenet, P.G., Roberts, M.R., 2007. Transneuronal mapping of the CNS network controlling sympathetic outflow to the rat thymus. Auton. Neurosci. 131, 9–20.
Uddman, R., Malm, L., Sundler, F., 1983. Substance-P-containing nerve fibers in the nasal mucosa. Arch Otorhinolaryngol. 238, 9–16.
Ueyama, T., Kozuki, K., Houtani, T., Ikeda, M., Kitajiri, M., Yamashita, T., Kumazawa, T., Nagatsu, I., Sugimoto, T., 1990. Immunolocalization of tyrosine hydroxylase and vasoactive intestinal polypeptide in nerve fibers innervating human palatine tonsil and paratonsillar glands. Neurosci. Lett. 116, 70–74.
Weihe, E., Eiden, L.E., 2000. Chemical neuroanatomy of the vesicular amine transporters. FASEB J. 14, 2435–2449.
Weihe, E., Krekel, J., 1991. The neuroimmune connection in human tonsils. Brain Behav. Immun. 5, 41–54.
Weihe, E., Schäfer, M.K., Erickson, J.D., Eiden, L.E., 1994. Localization of vesicular monoamine transporter isoforms (VMAT1 and VMAT2) to endocrine cells and neurons in rat. J. Mol. Neurosci. 5, 149–164.
Wiley, J.A., Tighe, M.P., Harmsen, A.G., 2005. Upper respiratory tract resistance to influenza infection is not prevented by the absence of either nasal-associated lymphoid tissue or cervical lymph nodes. J. Immunol. 175, 3186–3196.
Zuercher, A.W., Cebra, J.J., 2002. Structural and functional differences between putative mucosal inductive sites of the rat. Eur. J. Immunol. 32, 3191–3196.